Two Substrate Binding Sites in Ascorbate Peroxidase: The Role of Arginine 172†

Evan H. Bursey and Thomas L. Poulos*

Departments of Molecular Biology & Biochemistry and Physiology & Biophysics and the Program in Macromolecular Structure, University of California, Irvine, California 92697-3900

Received February 28, 2000; Revised Manuscript Received April 18, 2000

ABSTRACT: Site-directed mutagenesis has been used to probe the role of Arg172 in ascorbate utilization by ascorbate peroxidase. Arg172 was changed to lysine, glutamine, and asparagine. Although each of these variants retains the ability to utilize guaiacol as a reductant, they exhibit large decreases in their steady-state rates of ascorbate utilization. Spectroscopic, steady-state, and transient-state experiments indicate that these variant proteins are capable of reacting with hydrogen peroxide to form Compound I, but their ability to oxidize ascorbate to form Compound II, and subsequently the resting state, is severely impeded. Results are presented which highlight the importance of Arg172, and a model is proposed to explain its role in ascorbate utilization.

Cytosolic ascorbate peroxidase (APX)[1] from the leaves of the pea plant *Pisum sativum*, a 54 000 Da dimeric heme protein, is a member of the class I (prokaryotic) family of peroxidases according to the scheme proposed by Welinder (*1*). APX participates in the protection of the cell from hydrogen peroxide by catalyzing the reduction of hydrogen peroxide at the expense of ascorbate oxidation in the following reaction mechanism where S = ascorbate:

$$H_2O_2 + Fe^{3+}\,P \rightarrow H_2O + Fe^{4+}{=}O\,P^{\bullet}\ \text{(Compound I)}$$

$$Fe^{4+}{=}O\,P^{\bullet} + S \rightarrow S^{\bullet} + Fe^{4+}{=}O\,P\ \text{(Compound II)}$$

$$Fe^{4+}{=}O\,P + S \rightarrow S^{\bullet} + H_2O + Fe^{3+}\,P\ \text{(resting state)}$$

Hydrogen peroxide removes two electrons from the enzyme to give the $Fe^{4+}{=}O$ oxyferryl center and a porphyrin radical ($P^{\bullet}$) (*2*). The substrate for the above reaction in vivo is believed to be ascorbate (*3*), although, like other peroxidases, APX is somewhat promiscuous and is able to oxidize other small molecules such as guaiacol and pyrogallol. The site of interaction between the substrate and APX and other peroxidases is generally considered to be the exposed δ-edge of the heme. Hill et al. (*4*) studied the interaction between APX and ascorbate using modification of the heme by phenylhydrazine, estimation of iron−ascorbate distances as determined by nuclear magnetic resonance, and computer modeling. These authors concluded that ascorbate interacts with APX approximately 9 Å from the heme iron near the δ-heme edge which is consistent with the general view on how substrates interact with peroxidases. This also is the most obvious location for substrate interactions since the δ-heme edge is exposed in all known related peroxidase structures and the crystal structures of plant peroxidases such as horseradish peroxidase complexed with small aromatic substrates show binding near the δ-heme edge (*5*−*7*).

Evidence now is mounting, however, that the δ-edge is not the only substrate interaction site in peroxidases. The crystal structure of manganese peroxidase (MnP) revealed that its substrate, Mn^{2+}, interacts with several amino acids and one of the oxygen atoms of a heme propionate at the γ-heme edge (*8*). That this edge is, in fact, the site of substrate interaction has been further demonstrated by mutagenesis studies (*9*−*12*). In addition to the use of the δ-edge in horseradish peroxidase and the use of the γ-edge in MnP, it has also been reported that a tryptophan residue approximately 10 Å from the α-heme edge is important for the use of veratryl alcohol by lignin peroxidase (*13*). Recently we found that chemical modification of the Cys32 residue in APX with 5,5′-dithiobis(2-nitrobenzoic acid) (DTNB) near the γ-heme edge blocks ascorbate peroxidase activity but not guaiacol peroxidase activity. Figure 1 shows the relationship of Arg172 and Cys32 to the γ-heme edge. We hypothesized that the reason for the specific loss of ascorbate peroxidase activity resulted from the bulky TNB group attached to Cys32 blocking access to Arg172 which could possibly provide an electrostatic binding site for the negatively charged ascorbate anion near the γ-heme edge. The present study was designed to test the role of Arg172 using site-directed mutagenesis.

MATERIALS AND METHODS

Mutagenesis and Expression. Mutagenesis was initially performed using a PCR-based method and a previously described (*14*) plasmid construct, pMAPXZΔ15, that is based on the pMAL-C2 plasmid and codes for a fusion protein of maltose-binding protein and APX. The mutagenesis method consisted of two rounds of PCR using the pMAPXZΔ15 plasmid as a template and Pwo DNA polymerase (Boehringer Mannheim). The first round of PCR used one of two 23 base oligonucleotide primers designed to anneal to the template beyond either the 5′ or the 3′ end of the APX gene, depending

† This work was supported by NIH Grant GM42614.

* To whom correspondence should be addressed at the Department of Molecular Biology & Biochemistry, University of California, Irvine, CA 92697-3900. Fax: (949) 824-3280. Email: poulos@uci.edu.

[1] Abbreviations: APX, ascorbate peroxidase; DTNB, 5,5′-dithiobis-(2-nitrobenzoic acid); TNB, thiobis(2-nitrobenzoic acid).

10.1021/bi000446s CCC: $19.00
Published on Web 05/27/2000

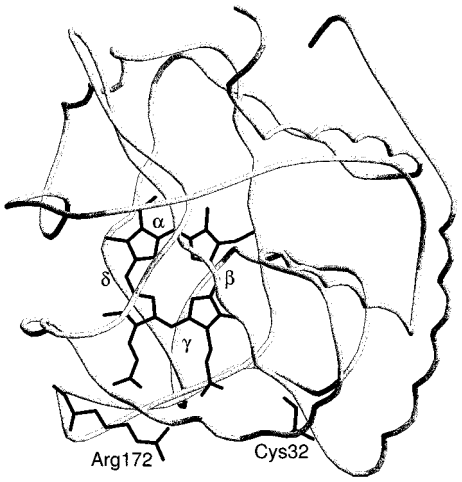

FIGURE 1: View of wild-type APX showing the position of the heme, Arg172, and Cys32. The four heme edges are labeled α, *β*, *γ*, and *δ* respectively. Molscript (*21*) and Raster3D (*22*) were used to produce this image.

on the specific mutation. The second primer contained the desired mutation and was designed to anneal around the mutation site on the strand opposite the first primer. The product of this reaction contained some flanking DNA and part of the APX gene with the desired mutation. Product was gel purified and used as a primer for the second PCR reaction along with a primer designed to anneal to the opposite strand of the template at the other end of the APX gene. The product of this second reaction consisted of the full-length APX gene with the desired mutation as well as flanking template DNA on both sides of the gene. The 5′ flanking DNA contained a unique *Sac*I restriction site, and the 3′ flanking DNA contained a unique *Xba*I restriction site. The PCR product was gel purified, restricted with *Xba*I and *Sac*I, and ligated into the pMAL-C2 vector to give a mutant pMAPXZΔ15 plasmid. The plasmid construct was sequenced to confirm the presence of the mutation by fluorescence-labeled dideoxy-sequencing at the UC Irvine Automated DNA Sequencing Facility. While easy to purify, difficulties arose while cleaving the fusion protein to give free APX. To avoid these difficulties, the wild-type and mutant APX genes were modified to encode a 6-histidine tag at the 5′ end of the gene and were cloned into the pTrc99a plasmid (Pharmacia). This was performed by PCR using the mutant pMAPXZΔ15 plasmids as templates. The PCR primers consisted of an oligonucleotide that annealed beyond the 3′ end of the APX gene and contained a unique *Hin*dIII restriction site and an oligonucleotide that annealed to the opposite DNA strand and was complementary to the 5′ end of the APX gene. The 5′ primer encoded the addition of Met-Ala-His_6-Arg to the N-terminus of the protein. The amino-terminal Met codon was part of a unique *Nco*I restriction site. The resulting PCR product was gel purified, restricted with *Nco*I and *Hin*dIII, and ligated into pTrc99a. This plasmid was transformed into the *E. coli* TOPP2 strain and expressed as previously described (*14*). After expression, the bacterial cultures were harvested by centrifugation, and the cell paste was stored at −70 °C.

The His-tagged APX protein was purified from the TOPP2 cells using the following procedure. Approximately 20 g of *E. coli* cell paste was thawed in a flask containing 1 volume of 50 mM $NaPO_4$, pH 7.8, 1.4 mM *β*-mercaptoethanol, 200 mM NaCl, 10 mM imidazole, 5% glycerol (column buffer). The cell paste was then frozen by immersing the flask in liquid nitrogen and thawed with the addition of 2 volumes of column buffer. The solution was made 1 mM PMSF, 0.5 mM EDTA, 5 mg/mL lysozyme and incubated with gentle shaking on ice for 1 h. The solution then was made 20 mM $MgCl_2$ and 50 *μ*g/mL DNase and incubated on ice with gentle shaking for 30 min. The solution was centrifuged at 27000*g* at 4 °C for 30 min followed by chromatography over a 3.5 × 2.5 cm Ni-NTA (Qiagen) column that had been preequilibrated with column buffer. The column was washed with column buffer containing 25 mM imidazole until the Abs_{280} of the eluate returned to baseline (between 150 and 300 mL). APX was eluted by washing the column with column buffer containing 200 mM imidazole. While essentially pure at this point, the protein was typically a mix of apo- and holo-protein. Heme incorporation was performed using a published method (*15*). The protein then was dialyzed against 50 mM KPO_4, pH 7.0, concentrated using a Centriprep 30, aliquoted, and stored at −70 °C until used.

Extinction Coefficient Determination. The Soret extinction coefficients of the wild-type and each of the mutants were determined using the hemochromogen method (*16*).

Kinetics. Steady-state and transient-state kinetic assays were performed as previously described (*17*), with the exception that 1 mM EDTA was used instead of 0.1 mM EDTA.

RESULTS

Spectral Properties. The wild-type and variant proteins were initially purified as a mixture of apo- and holo-proteins, and therefore required heme incorporation. Following heme incorporation, the R172Q variant had an increased reinheitzahl (RZ) number relative to the wild-type value. While a decreased RZ number would be easy to dismiss as being due to incomplete heme incorporation, an increase was more difficult to explain. The protein was dialyzed against 200 mM imidazole in an attempt to remove any heme that might be associated with the amino-terminal histidine tail. This dialysis resulted in a small decrease in the RZ number, but the number could not be decreased further. Furthermore, hemochromogen assays indicated a 1:1 ratio of heme to APX monomer (as determined using an ϵ_{280} of 44 mM^{-1} cm^{-1}), so we proceeded under the assumption that the increased Soret peak was due to a change in the spectrum rather than any associated free heme. Since the Soret absorbance is used to quantitate holoenzyme concentration for activity assays, the possibility that the mutations might affect the visible absorbance spectra in these variants was of some practical concern. To address this concern, the Soret extinction coefficient was determined for the wild-type and each of the variant proteins. The values of 10×10^4, 11.3×10^4, 10.6×10^4, and 11.7×10^4 M^{-1} cm^{-1} for the wild-type, R172N, R172Q, and R172K proteins, respectively, were used in subsequent concentration calculations. As seen in Figure 2, the spectra of the variants are virtually identical to the wild-type, with the exception of the intensity of the Soret peak relative to the protein peak at 280 nm, suggesting that there are subtle changes but no gross abnormalities around the heme.

When hydrogen peroxide is added to APX, the iron and the heme are oxidized to Compound I which gives a

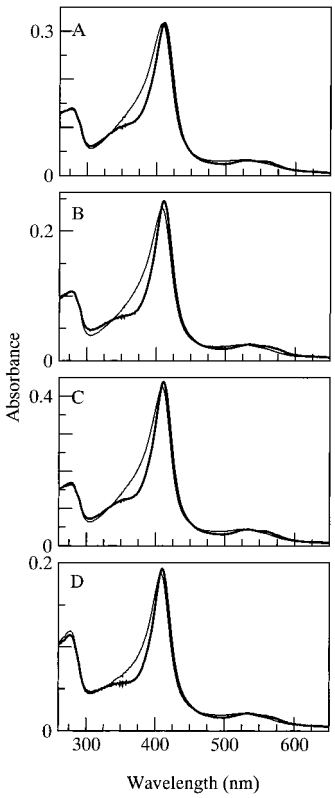

FIGURE 2: UV−visible spectra of wild-type (A), R172N (B), R172Q (C), and R172K (D) APX in the resting state (thin lines) and in the Compound II state (thick lines). Proteins were diluted in 50 mM KPO_4, pH 7.0. Compound II was formed by adding 4 molar equiv of hydrogen peroxide.

porphyrin radical and Fe^{4+}═O. Compound I, however, is relatively short-lived, and the porphyrin radical rapidly decays, leaving the oxyferryl Compound II. Figure 2 shows the absorbance spectra of the wild-type and the three variant proteins when mixed with hydrogen peroxide. All three variants exhibit a Compound II absorbance spectrum that is qualitatively similar to that of the wild-type protein, indicating that these variants are able to react normally with hydrogen peroxide to form Compound II.

Rate of Compound I Formation. The rate of Compound I formation was monitored using stopped-flow spectroscopy. The dependence of the observed rates of Compound I formation vs hydrogen peroxide concentration is shown in Figure 3, and the resulting second-order rate constants for the wild-type and the variant proteins are listed in Table 1. These results indicate that the wild-type and variant proteins react with hydrogen peroxide at very similar rates, which further indicates that the catalytic machinery required for rapid formation of Compound I is not affected in the mutants.

Rate of Compound II Formation. Compound II formation was also monitored using stopped-flow spectroscopy. A mixture of ascorbate and hydrogen peroxide was placed in one syringe, and APX was placed in the second syringe. Hydrogen peroxide was present in excess to rapidly drive the formation of Compound I to completion and force the subsequent Compound II formation into pseudo-first-order kinetics. The reduction of Compound I by ascorbate then was monitored by measuring the decrease in the absorbance at 424 nm. As depicted in Figure 4, the dependence of the rate of Compound II formation does not increase linearly

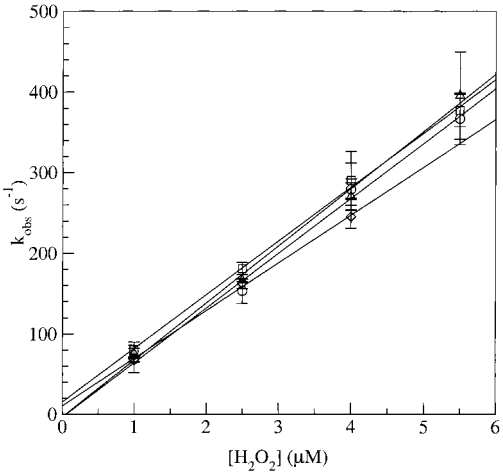

FIGURE 3: Transient-state kinetics of Compound I formation of wild-type (○), R172N (◇), R172Q (△), and R172K (□) APX. The concentration of APX was 2 μM, and the reaction was carried out at 21 °C by following the change in absorbance at 411 nm.

with increasing ascorbate concentration. This indicates that the reaction is not behaving like a first-order process, and, therefore, for the purposes of comparing the wild-type activity with that of the variants, we have determined the slope of the initial part of each curve and have reported these as percent wild-type activity in Table 1. The variant proteins each exhibit a marked decrease in their ability to utilize ascorbate as a source of reducing equivalents, indicating that the replacement of the Arg172 side chain disrupts the ability of APX to accept electrons from ascorbate.

Compound II Reduction. The final, and rate-limiting, step in the reaction cycle is the reduction of Compound II back to the resting state. This process was monitored using stopped-flow spectroscopy to follow the change in absorbance at 421 nm. Compound II was formed by mixing equimolar amounts of APX and hydrogen peroxide and allowing the solution to age for a few minutes. The Compound I solution was placed in one syringe, and a solution of ascorbate was placed in the other. Figure 5 shows how the rate of Compound II reduction changes with increasing ascorbate concentration. Unfortunately, like Compound II formation, Compound II reduction does not follow simple first-order kinetics, nor are the kinetics truly hyperbolic. For this reason, the data were not fitted to any sort of kinetic model. Instead, the initial slope of each curve was determined, and these values are reported in Table 1 as percent wild-type activity. Also shown in Figure 5 are typical stopped-flow traces for the wild-type and R172K proteins. It is interesting to note that the traces for the variants differ from the wild-type. In particular, an immediate increase in absorbance, followed by a lag are observed for the variants prior to the exponential decay phase. It is unclear whether this difference is part of the normal catalytic cycle but is only observed here because the reaction has been slowed, or if this represents some abnormal step that has been introduced into Compound II reduction. In the case of the variants, the rate data were extracted by selecting the part of each curve which best fit the exponential decay model. Figure 5 clearly shows that the rate of Compound II reduction by ascorbate is dramatically decreased in each of the variant proteins. This decreased activity supports the idea that replacement of the Arg172 side chain disrupts APX's ability

Table 1: Transient-State and Steady-State Rates of Wild-Type and Variant Proteins

	Compound I formation (M^{-1} s^{-1})	Compound II formation (% wild-type)	Compound II reduction (% wild-type)	ascorbate steady-state (% wild-type)	guaiacol steady-state V_{max} (s^{-1}), K_m (mM)
wild-type	68.0×10^6	100	100	100	39.9, 9.3
R172N	59.2×10^6	20	3.5	6.6	47.0, 12.4
R172Q	70.9×10^6	19	4.5	4.4	51.4, 5.6
R172K	66.7×10^6	37	5.0	15.2	99.6, 11.7

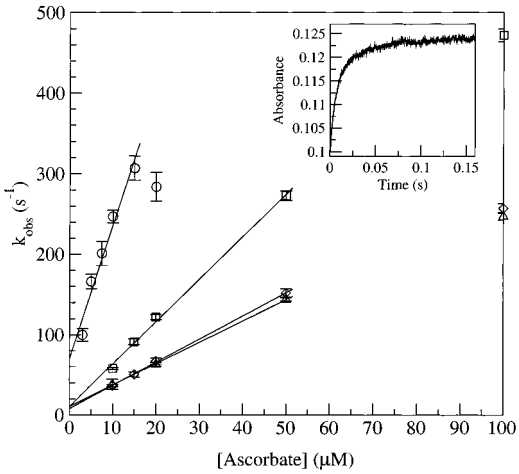

FIGURE 4: Transient-state kinetics of Compound II formation of wild-type (○), R172N (◇), R172Q (△), and R172K (□) APX. The inset shows a typical wild-type stopped-flow trace. The concentrations of hydrogen peroxide and APX were 25 μM and 2 μM, respectively, and the reaction was carried out at 21 °C by monitoring the absorbance at 424 nm.

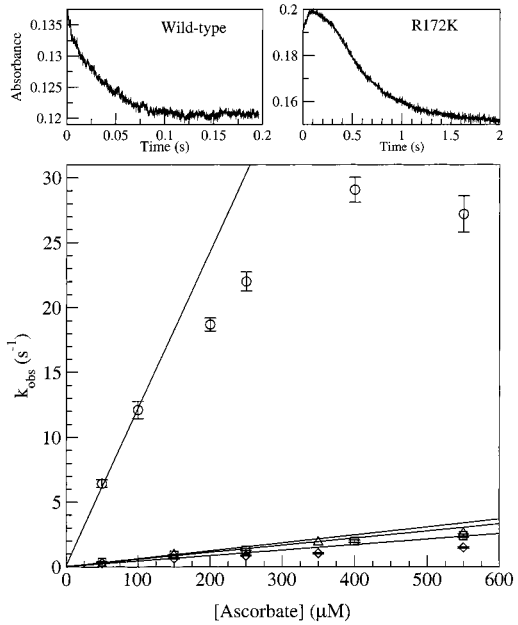

FIGURE 5: Transient-state kinetics of Compound II reduction of wild-type (○), R172N (◇), R172Q (△), and R172K (□) APX. The two graphs at the top of the figure show typical stopped-flow traces for the wild-type and R172K proteins. The concentration of both hydrogen peroxide and APX was 2 μM. The reaction was followed at 421 nm and was carried out at 23 °C.

to utilize ascorbate as a source of electrons, and furthermore suggests that ascorbate interacts with the protein in the same way during both Compound I and Compound II reduction.

Steady-State Ascorbate Activity. Figure 6 depicts the rate of ascorbate oxidation as a function of ascorbate concentration. The ascorbate peroxidase activity of APX is known not to exhibit Michaelis−Menten kinetics (*17*). In addition, it is apparent from Figure 6 that the observed rates of wild-type and variant proteins display saturation with increasing ascorbate concentration. For the purpose of comparison, the slope of the initial part of the activity curve was measured and is reported as percent maximum wild-type activity in Table 1. These results correlate well with the transient-state kinetics, and indicate that the variant APX proteins are impaired in their ability to use ascorbate as a reductant. The relative rates listed in Table 1 must be viewed with some caution. For instance, the R172K steady-state rate is about 15% of the wild-type rate. However, its rate-limiting step (Compound II reduction) is only 5% the wild-type rate. This apparent inconsistency is most likely related to the fact that APX oxidation of ascorbate does not obey simple Michaelis−Menten kinetics. Without a suitable kinetic model, it is not possible to dissect out a true catalytic rate constant. Therefore, we report relative activities based on initial slopes which are subject to large errors, especially in the transient-state experiments measuring Compound II reduction.

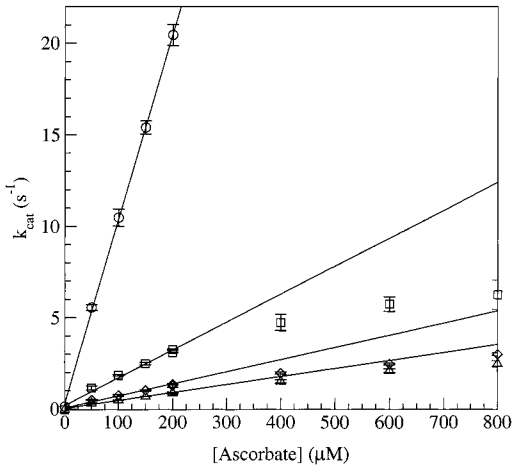

FIGURE 6: Ascorbate oxidation by wild-type (○), R172N (◇), R172Q (△), and R172K (□) APX. APX concentrations were 30, 1480, 1500, and 329 nM, respectively.

Despite these uncertainties, it is worth noting that both the steady-state assay and the single-turnover Compound II reduction assay exhibit the same nonhyperbolic dependence on ascorbate concentration and both saturate at similar ascorbate concentrations. In addition, the predicted steady-state rate from the Compound II reduction data is very close to 60−70 s^{-1} (unpublished). The maximum Compound II reduction rate is about 28 s^{-1}, which predicts a steady-state rate of about 56 s^{-1} since in the steady-state reaction two ascorbate molecules are oxidized per cycle while in the stopped-flow experiment only one ascorbate molecule is

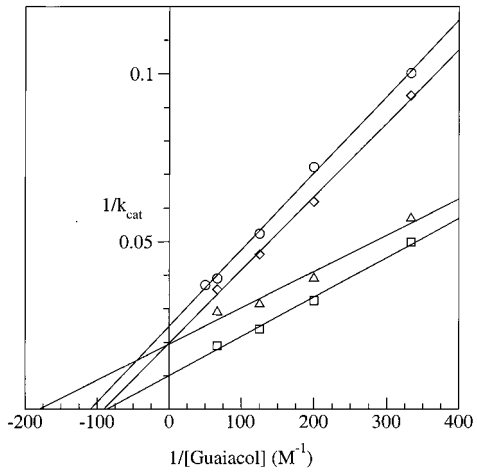

FIGURE 7: Guaiacol oxidation by wild-type (○), R172N (◇), R172Q (△), and R172K (□) APX. APX concentrations were 30, 13.6, 31.9, and 19.8 nM, respectively.

oxidized. This demonstrates that the reduction of Compound II is rate-limiting under steady-state conditions.

Steady-State Guaiacol Activity. Like other peroxidases, APX is able to use other molecules as a source of electrons during turnover. One such reductant is the phenolic compound guaiacol. To determine the effect that these mutations might have on the ability of APX to accept electrons from guaiacol, steady-state guaiacol turnover experiments were performed. Unlike ascorbate, guaiacol reduction follows Michaelis−Menten kinetics, thus enabling the estimation of V_{max} and K_m. The results of these experiments are presented in Table 1, and the Michaelis−Menten-type kinetics are illustrated in Figure 7. Interestingly, the variants showed no decrease in activity when guaiacol was used as a reductant. Therefore, it appears that Arg172 is required for the oxidation of ascorbate but not guaiacol.

DISCUSSION

Work previously published by this laboratory demonstrated that chemical modification of the single Cys residue in APX by TNB resulted in a protein that is unable to use ascorbate to support peroxidase activity (*17*). X-ray crystallography was used to show that TNB is covalently bound to the sulfur atom of a single cysteine residue, Cys32 (Figure 1). This cysteine is near the γ-heme edge with its side chain pointed into a hydrophobic pocket. However, after modification by TNB, the Cys32 side chain reorients itself in such a way that it and the attached DTNB stretch across the γ-heme edge and the DTNB carboxyl group hydrogen bonds to the nearby Arg172. One possible explanation for the resulting loss of ascorbate peroxidase activity is that the γ-heme edge is the site where electrons are accepted from ascorbate, and that steric blocking of this edge by the Arg172-TNB-Cys32 group prevents the proper approach of the ascorbate molecule. Another possibility is that Arg172 is somehow important not only for binding but also for the electron-transfer process. Since ascorbate is an anion at neutral pH, Arg172 might provide an electrostatic substrate binding site. That electrostatics are involved is evidenced by the fact that ascorbate peroxidase but not guaiacol peroxidase activity decreases in high salt (*17*). If steric access to the γ-heme edge were the only basis for loss in activity in the TNB-modified enzyme,

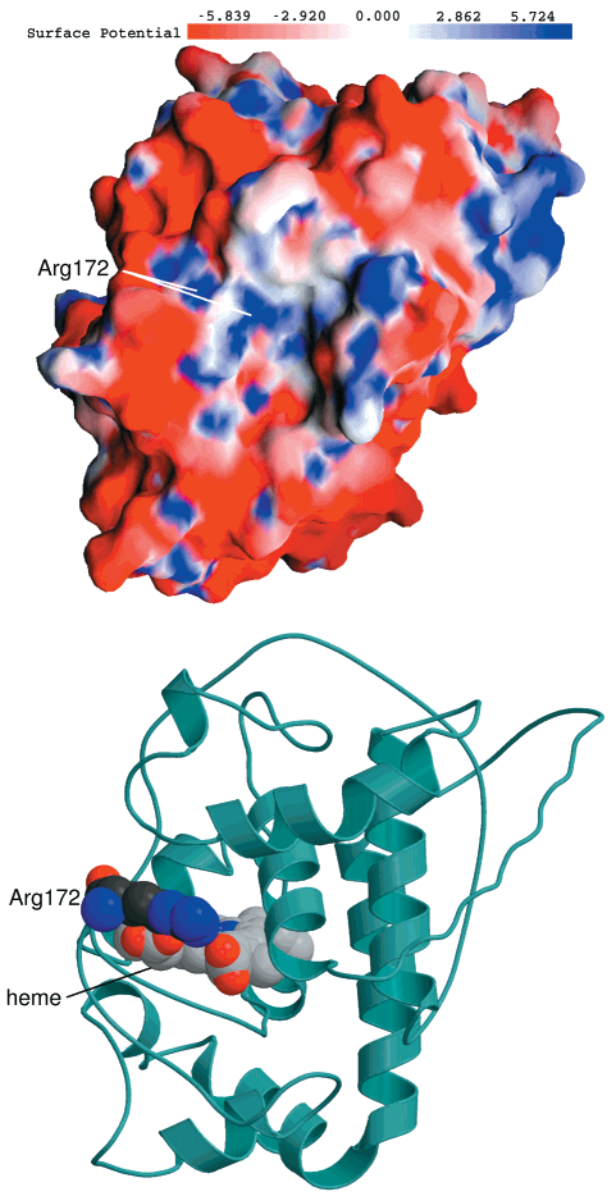

FIGURE 8: Structure of APX. The upper panel depicts the calculated electrostatic potential at the surface of the protein. The lower panel is included for clarity and depicts the APX protein in approximately the same orientation. The figure was prepared using Grasp (upper panel) (*23*) and a combination of Molscript (*21*) and Raster3D (*22*) (lower panel).

then replacement of Arg172 with glutamine, asparagine, or lysine should not lead to a loss in activity. Therefore, our present results support a more direct role for Arg172 in ascorbate binding and oxidation.

Figure 8 shows the electrostatic surface potential of APX. The electrostatic potential, due primarily to Arg172, is positive near the γ-heme edge while the surrounding protein exhibits a negative electrostatic potential. As a result, the negatively charged ascorbate anion might electrostatically dock near Arg172. Replacing Arg172 with neutral side chains would substantially decrease the ability of ascorbate to bind. Here it is interesting to note that the R172K mutant, while still exhibiting much lower activity, does exhibit between 2 and 3 times more steady-state activity than the R172N and R172Q mutants. The positively charged lysine side chain

may be able to partially compensate for arginine. The inability of the R172K mutant to generate full activity may be due to an altered conformation of the side chain, especially if a direct H-bonding interaction between ascorbate and Arg172 is required for optimal activity. There also is the possibility that Arg172 might perform a direct function by serving as an electron-transfer conduit between ascorbate and the heme propionate. Utilization of heme propionates for this purpose is not without precedence since the substrate of manganese peroxidase, Mn^{2+}, directly coordinates to a heme propionate prior to oxidation to Mn^{3+} by Compound I. More recently it has been proposed that the pterin cofactor in nitric oxide synthase transfers an electron via a heme propionate to the heme iron during the oxygen activation step of the reaction (*18*−*20*). In the wild-type structure of APX, Arg172 is about 3.7 Å from the heme propionate, so some adjustments would be required in the substrate complex in order for Arg172 to provide a direct hydrogen bonding link to the heme. While the possible role of Arg172 in electron transfer remains speculative, the present study does support the role of Arg172 in providing an electrostatic site for ascorbate binding. Hence, as we previously hypothesized, APX has two distinct substrate binding sites: one for neutral aromatic phenols and one for the ascorbate anion. These results are particularly interesting in light of the recent findings that manganese peroxidase may have two substrate binding sites (*10*, *11*) and lignin peroxidase may also have a specialized site for its natural substrate, veratryl alcohol (*13*). Taken together, these studies challenge the conventional view that peroxidases bind and react with small substrates at the exposed heme edge. Thus far, manganese, lignin, and ascorbate peroxidase have been shown to utilize such specialized sites, and it will be most interesting to learn if other related peroxidases also have unique sites for their natural substrates.

REFERENCES

1. Welinder, K. G. (1992) *Curr. Opin. Struct. Biol. 2*, 388−393.
2. Patterson, W. R., Poulos, T. L., and Goodin, D. B. (1995) *Biochemistry 34*, 4342−4345.
3. Nakano, Y., and Asada, K. (1981) *Plant Cell Physiol. 33*, 867−880.
4. Hill, A. P., Modi, S., Sutcliffe, M. J., Turner, D. D., Gilfoyle, D. J., Smith, A. T., Tam, B. M., and Lloyd, E. (1997) *Eur. J. Biochem. 248*, 347−354.
5. Henriksen, A., Schuller, D. J., Meno, K., Welinder, K. G., Smith, A. T., and Gajhede, M. (1998) *Biochemistry 37*, 8054−8060.
6. Henriksen, A., Smith, A. T., and Gajhede, M. (1999) *J. Biol. Chem. 274*, 35005−35011.
7. Tsukamoto, K., Itakura, H., Sato, K., Fukuyama, K., Miura, S., Takahashi, S., Ikezawa, H., and Hosoya, T. (1999) *Biochemistry 38*, 12558−12568.
8. Sundaramoorthy, M., Kishi, K., Gold, M. H., and Poulos, T. L. (1994) *J. Biol. Chem. 269*, 32759−32767.
9. Sollewijn Gelpke, M. D., Moënne-Loccoz, P., and Gold, M. H. (1999) *Biochemistry 38*, 11482−11489.
10. Kusters-van Someren, M., Kishi, K., Lundell, T., and Gold, M. H. (1995) *Biochemistry 34*, 10620−10627.
11. Kishi, K., Kusters-van Someren, M., Mayfield, M. B., Sun, J., Loehr, T. M., and Gold, M. H. (1996) *Biochemistry 35*, 8986−8994.
12. Whitwam, R. E., Brown, K. R., Musick, M., Natan, M. J., and Tien, M. (1997) *Biochemistry 36*, 9766−9773.
13. Doyle, W. A., Blodig, W., Veitch, N. C., Piontek, K., and Smith, A. T. (1998) *Biochemistry 37*, 15097−15105.
14. Patterson, W. R., and Poulos, T. L. (1994) *J. Biol. Chem. 269*, 17020−17024.
15. Fishel, L. A., Villafranca, J. E., Mauro, M., and Kraut, J. (1987) *Biochemistry 26*, 351−360.
16. Paul, K. G., Theorell, H., and Åkeson, Å. (1953) *Acta Chem. Scand. 7*, 1284−1287.
17. Mandelman, D., Jamal, J., and Poulos, T. L. (1998) *Biochemistry 37*, 17610−17617.
18. Bec, N., Gorren, A. C. F., Voelker, C., Mayer, B., and Lange, R. (1998) *J. Biol. Chem. 273*, 13502−13508.
19. Raman, C. S., Li, H., Martásek, P., Král, V., Masters, B. S. S., and Poulos, T. L. (1998) *Cell 95*, 939−950.
20. Hurshman, A. R., Krebs, C., Edmondson, D. E., Huynh, B. H., and Marletta, M. A. (1999) *Biochemistry 38*, 15689−15696.
21. Kraulis, P. J. (1991) *J. Appl. Crystallogr. 24*, 946−950.
22. Merritt, E. A., and Bacon, D. J. (1997) *Methods Enzymol. 277*, 505−524.
23. Sharp, K., Fine, R., and Honig, B. (1987) *Science 236*, 1460−1463.

BI000446S